Proceedings of the 17th World Congress
The International Federation of Automatic Control
Seoul, Korea, July 6-11, 2008

An estimation process for vehicle wheel-ground contact normal forces

Moustapha Doumiati, Alessandro Victorino, Ali Charara, Guillaume Baffet [*] **Daniel Lechner** [**]

[*] *Heudiasyc Laboratory UMR CNRS 6599, Université de Technologie de Compiègne UTC, BP20529-60205 Compiègne, France (mdoumiat@hds.utc.fr, acorreav@hds.utc.fr, acharara@hds.utc.fr, baffetgu@hds.utc.fr)*

[**] *INRETS-MA Laboratory Departement of Accident Mechanism Analysis, Chemin de la Croix Blanche, 13300 Salon de Provence, France (daniel.lechner@inrets.fr)*

Abstract: This paper presents a new methodology for estimating wheel-ground contact normal forces, commonly known as vertical forces. The proposed method uses measurements from currently available standard sensors (accelerometers and relative suspension sensors). The aim of this study is to improve vehicle safety, especially to prevent rollover problems. One particular feature of the method is the separation of the estimation process into three blocks. The first block serves to identify the vehicle's weight, the second block contains a linear observer whose main role is to estimate the one-side lateral transfer load, while the third block calculates the four wheel vertical forces using a nonlinear observer. The different observers are based on the Kalman filter. The estimation process is applied and compared to real experimental data obtained in real conditions. Experimental results validate and prove the feasibility of this approach.

NOTATIONS

a_x, a_y	longitudinal and lateral acceleration occurs at the cog in the inertiel coordinate system m/s^2
a_{ym}	measured lateral acceleration m/s^2
e_f, e_r	front and rear vehicle's track respectively m
Fz_l	vertical load on the left tires N
Fz_r	vertical load on the right tires N
Fz_F	vertical load on the front tires N
Fz_R	vertical load on the rear tires N
Fz_{ij}	vertical load on each wheel N
k_f, k_r	front and rear roll stiffness respectively $N.m/rad$
k_s, k_t	spring and tire stiffness respectively N/m
g	gravitational constant 9.81 m/s^2
h	height of the center of gravity m
h_f, h_r	height of the front and rear roll respectively m
i	front(f) or rear(r)
j	Left(l) or right(r)
l_f, l_r	distance from the cog to the front and rear axles respectively m
m_{ij}	quarter mass of the vehicle on each corner of the vehicle kg
m_{eij}	quarter mass of the empty vehicle on each corner of the vehicle kg
m_v	total mass of the vehicle kg
m_s	sprung mass kg
ΔFz_l	lateral transfer load applied to the left part of the vehicule N
ΔFz_r	lateral transfer load applied to the right part of the vehicule N
Δm_{sij}	variation of the sprung mass on each corner of the vehicle m
θ	roll angle rad
δ_{ij}	suspension deflection on each vehicle's corner
X	$X = [x_1\ x_2\ ...\ x_n]$ is the state space vector
Z	$Z = [z_1\ z_2\ ...\ z_m]$ is the observation vector

1. INTRODUCTION

The automotive industry has made significant technological progress over the last decade in the development of on-board control systems, in order to improve security and help to prevent dangerous situations. Among these controllers, we find systems such as Anti-lock Braking Systems (ABS) and Electronic Stability Programs (ESP). Improving control decisions is possible when certain vehicle parameters, such as velocity, roll angle, yaw rate, sideslip angle, vehicle's weight, and wheel ground forces are known. Due to technical, physical and economic reasons, some of these parameters are not measurable in a standard vehicule. For example, measuring vertical tire forces requires wheel transducers that cost 100.000 €. The knowledge of wheel-ground contact normal forces is essential for improving transportation security. Indeed, vertical load on the tire has a primary influence on vehicle stability and cornering stiffness, which in turn determines the lateral force. Moreover, on-line measurement of vehicle tire forces, in a moving vehicle, allows a better calculation of the road damage or Lateral Transfer Ratio (LTR) parameter. LTR is an indicator used to prevent or forecast rollover situations. The LTR coefficient is defined as the ratio of the difference between the sum of the left wheel loads and the right wheel loads, to the sum of all the wheel loads. LTR is estimated in this article.

The estimation of the vertical tire load is considered a difficult task. The variation of the vehicles mass, the position of the center of gravity (cog), the road grade, the road irregularities and the load transfer increase the problem's complexity.

In the literature, many studies deal with the calculation of the wheel-ground contact normal forces. In Lechner (2002), the author presented a model for vertical force calculation. Lechner's model respects the superposition principle, assuming independent longitudinal and lateral

acceleration contributions. In Shim et al. (2007), a study of a 14 DOF (Degree Of Freedom) vehicle model is proposed where the dynamics of the roll center are used to calculate vertical tire forces. In the work of Nielson et al. (2000), the tire forces are modeled by coupling longitudinal and lateral acceleration. Wenzel et al. (2006) investigated the application of the DEKF (Dual Extended Kalman Filter) for estimating vertical forces. They concluded that the obtained result differs from the reference data, the discrepancy being attributable to the problem of the vehicle's mass.

In this paper, our main objective is to develop a real-time method for estimation of the wheel-ground contact vertical forces, regardless of tire model, while taking into account the constraints of the industrial applicability. To simplify the model, pitch angle, road angle and road irregularities are not considered in our study. All notations presented in the following sections are included in the *notations* part.

The rest of the paper is organized as follows. The second section describes our algorithm. In the third, fourth and fifth sections, we describe each block of the estimation process. The sixth section presents an observability analysis. The seventh section presents experimental results of the evaluation of the observers with respect to real data. Finally, some concluding remarks are given in section 8.

2. DESCRIPTION OF THE ALGORITHM

The estimation process is modeled in three blocks as shown in Fig.1. The first block identifies the vehicle's mass at rest and calculates the static load applied to the vehicle. The identified mass will be used as a known vehicle parameter in the other blocks. The aim of the second block is to calculate the one-side lateral transfer load by using roll dynamics. The estimated value will be considered as an essential measure for the third block; it guarantees its observability. The third block estimates the four vertical tire forces, and serves to calculate the LTR coefficient. Each block will be described in detail in the following sections. The strategy of using cascaded observers allows us to avoid the observability problems entailed by an inappropriate use of the complete modeling equations, thus enabling then the estimation process to be carried out in a simple and practical way.

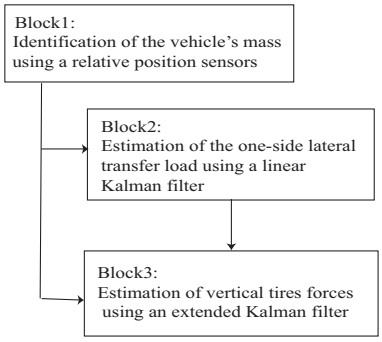

Fig. 1. Description of the three-block estimation process.

3. BLOCK 1: IDENTIFICATION OF THE VEHICLE'S MASS

Vehicle mass is a problem seldom discussed in the literature. For example, in Vahidi et al. (2005), a recursive least-squares method is developed for online estimation of vehicle mass. This method cannot be effective in our application because it takes a considerable time to converge to the real mass value. The objective of this section is to identify the vehicle's mass, *at rest*, by considering a quater-car model (Fig.2) and applying relative position sensors. Nowadays, many controlled suspensions are equipped with relative position sensors, which measure suspension deflections δ_{ij} (relative positions of the wheels with respect to the body) at each corner. The quarter mass

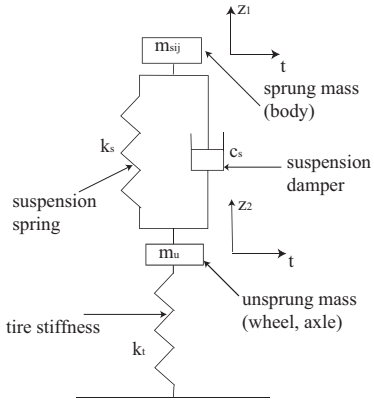

Fig. 2. A quarter car-model with linear suspension.

m_{eij} (sum of the sprung and unsprung masses) at each corner of the empty vehicle, is an information provided by the manufacturer. At a conventional suspension without level regulation and with linear spring characteristics, and by neglecting the wheel deflection, a load variation in the sprung mass Δm_{sij} changes the spring deflection $\delta_{ij} \rightarrow \delta_{ij} + \Delta ij$ where

$$\Delta m_{sij} = \frac{k_s \Delta_{ij}}{g}, \tag{1}$$

Δ_{ij} is the spring deflection variation. Then, the total quarter mass and the total mass of the vehicle is calculated as follows:

$$\begin{cases} m_{ij} &= m_{eij} + \Delta m_{sij} \\ m_v &= \sum_{i,j} m_{ij} \end{cases} \tag{2}$$

By using this identification method, the calculated mass converges to within $\pm 1\%$ error of the real mass value. As a consequence, when the vehicle is at rest, the static load applied at each wheel is equal to $m_{ij}g$.

4. BLOCK 2: OBSERVER FOR LATERAL TRANSFER LOAD

This section describes the first observer of our cascaded structure. It is based on the vehicle's roll dynamics. The roll angle of the vehicle is the amount of rotation of the vehicle's sprung mass about its roll axis, as shown in Fig.3 (see Anderson (2006)). During cornering, roll angle depends on the roll stiffness of the axle and on the position of the roll center. The roll axis is the line which passes through the roll center at the front and rear axel. Roll center can be constructed from the lateral motion of the wheel contact points (Milliken et al. (1995)).

In reality the roll center of the vehicle does not remain constant, but in this study a stationary roll center is assumed in order to simplify the model. The simplified equation for the lateral transfer load applied to the left

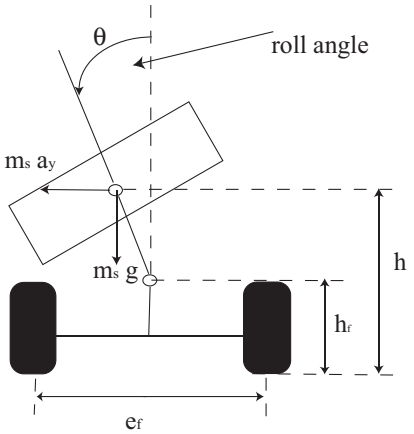

Fig. 3. Roll dynamic model (front view).

part of the vehicle can be formulated as the following dynamic relationship (Milliken et al. (1995)):

$$\begin{aligned}\Delta Fz_l &= (Fz_{fl} + Fz_{rl} - Fz_{fr} - Fz_{rr}) \\ &= (m_{fl} + m_{rl} - m_{fr} - m_{rr})g - 2(\frac{k_f}{e_f} + \frac{k_r}{e_r})\theta \\ &\quad -2\frac{m_s a_y}{l}(\frac{l_r h_f}{e_f} + \frac{l_f h_r}{e_r})\end{aligned} \quad (3)$$

The lateral acceleration used in equation (3) is generated at the cog. The accelerometer, however, is unable to distinguish the acceleration caused by the vehicle's motion from the gravitional acceleration. In fact, the measured quantity is a combination of the gravitational force and the acceleration of the vehicle as represented in the following equation(case of small roll angle):

$$a_{ym} = a_y + g\theta \quad (4)$$

In order to measure the roll angle, additional sensors are required and it is hard or very expensive to measure it. In this study, we consider that the roll angle can be calculated through relative suspension sensors (Brown et al. (2004); Rao (2005)). During cornering on a smooth road, the suspension is compressed on the outside and extended on the inside of the vehicle. By neglecting pitch dynamic effects on roll motion, the roll angle can be calculated by applying the following equation based on the geometry of the roll motion:

$$\theta = \frac{(\delta_{fl} - \delta_{fr} + \delta_{rl} - \delta_{rr})}{(2e_f)} - \frac{m_v a_{ym} h}{k_t} \quad (5)$$

4.1 The lateral transfer load estimation

By combining the relations (3), (4) and (5), a linear observer is developed to estimate the one-side lateral load transfer. The linear model with unknown inputs is:

$$\begin{cases} \dot{X}(t) = AX(t) + \alpha(t) \\ Z(t) = CX(t) + \beta(t) \end{cases} \quad (6)$$

- $X = \left[\Delta Fz_l\ \Delta Fz_r\ a_y\ \dot{a_y}\ \theta\ \dot{\theta}\right]$ is the state vector; the initial state vector is
  $X_0 = (m_{fl} + m_{rl} - m_{fr} - m_{rr})g\ -(m_{fl} + m_{rl} - m_{fr} - m_{rr})g\ 0\ 0\ 0\ 0]$.
- $Z = \left[a_{ym}\ (\Delta Fz_l + \Delta Fz_r)\ \theta\ \dot{\theta}\ \Delta Fz_l\right]$ is the observation vector where:
  - a_{ym}: lateral acceleration measured from the acceloremeter;
  - $\Delta Fz_l + \Delta Fz_r$: sum of right and left transfer load is supposed to be null at each instant;
  - θ: roll angle calculated by using equation (5);
  - $\dot{\theta}$: roll rate measured directly from gyrometer;
  - ΔFz_l: left transfer load calculated from equation (3).
- $\alpha(t)$ and $\beta(t)$ are the process and measurement noise vectors respectively, assumed to be white, zero mean and uncorrelated.

The constant matrices A and C are given as:

$$A = \begin{pmatrix} 0\ 0\ 0 & -2\frac{m_s}{l}(\frac{l_r h_f}{e_f} + \frac{l_f h_r}{e_r}) & 0 & -2(\frac{k_f}{e_f} + \frac{k_r}{e_r}) \\ 0\ 0\ 0 & 2\frac{m_s}{l}(\frac{l_r h_f}{e_f} + \frac{l_f h_r}{e_r}) & 0 & 2(\frac{k_f}{e_f} + \frac{k_r}{e_r}) \\ 0\ 0\ 0 & 1 & 0 & 0 \\ 0\ 0\ 0 & 0 & 0 & 0 \\ 0\ 0\ 0 & 0 & 0 & 1 \\ 0\ 0\ 0 & 0 & 0 & 0 \end{pmatrix}$$

$$C = \begin{pmatrix} 0\ 0\ 1\ 0\ g\ 0 \\ 1\ 1\ 0\ 0\ 0\ 0 \\ 0\ 0\ 0\ 0\ 1\ 0 \\ 0\ 0\ 0\ 0\ 0\ 1 \\ 1\ 0\ 0\ 0\ 0\ 0 \end{pmatrix}$$

5. BLOCK 3: ESTIMATION OF THE WHEEL GROUND VERTICAL CONTACT FORCES

Due to the longitudinal and lateral acceleration of the vehicule, the load distribution can significantly vary during a journey. The force due to the longitudinal acceleration at the cog causes a pitch torque which increases the rear axle load and reduces the front axle load. In addition, during cornering the lateral acceleration causes a roll torque which increases the load on the outside and decreases it on the inside of the vehicle (see Nielson et al. (2000)).
The load distribution can be expressed by the vertical forces that act on each of the four wheels (see Fig.4). These equations are:

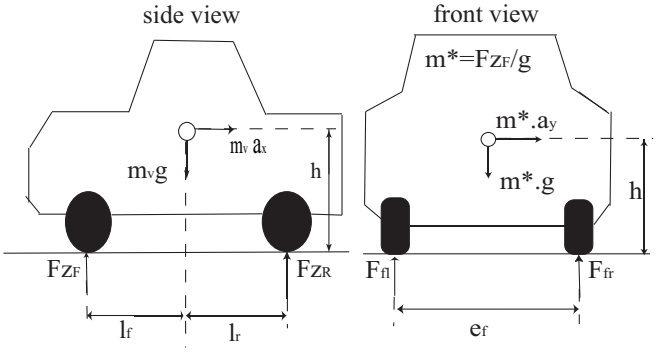

Fig. 4. Load shifting (acceleration+cornering).

$$\begin{cases} Fz_{fl,fr} = \frac{1}{2}m_v\left(\frac{l_r}{l}g - \frac{h}{l}a_x\right) \pm m_v\left(\frac{l_r}{l}g - \frac{h}{l}a_x\right)\frac{h}{e_f g}a_y \\ Fz_{rl,rr} = \frac{1}{2}m_v\left(\frac{l_f}{l}g + \frac{h}{l}a_x\right) \pm m_v\left(\frac{l_f}{l}g + \frac{h}{l}a_x\right)\frac{h}{e_r g}a_y \end{cases} \quad (7)$$

Having calculated these forces, we can then calculate the LTR coefficient and alert the driver in rollover situations. The LTR is defined in Boettiger et al. (2003) as:

$$LTR = \frac{Fz_l - Fz_r}{Fz_l + Fz_r} = \frac{\Delta Fz_l}{Fz_l + Fz_r}. \quad (8)$$

The value of LTR varies from -1 at the lift-off of the left wheel, tends toward 0 at no load transfer, and to 1 at the lift-off of the right wheel.

5.1 Estimation of the vertical forces at the wheel ground interaction

Using relations (7) and the estimated results from block 1, an extended Kalman filter (EKF) is constructed to estimate the four wheel-ground contact normal forces. The EKF has been applied and described in many studies especially in robotics field (see Durrant-Whyte (2001)). The evolution model is non-linear with unknown inputs :

$$\dot{X}(t) = f(X(t)) + \alpha(t) \quad (9)$$

Where $X = [Fz_{fl}\ Fz_{fr}\ Fz_{rl}\ Fz_{rr}\ a_x\ \dot{a}_x\ a_y\ \dot{a}_y]$ is the vehicle state vector and $\alpha(t)$ is the process noise assumed to be white with zero mean. The particular nonlinear functions of the state equation are then given by:

$$\begin{cases} f_1 = \frac{-h}{2l} m_v x_6 - m_v \frac{l_r h}{le_f} x_8 + m_v \frac{h^2}{le_f g} x_5 x_8 \\ \quad + m_v \frac{h^2}{le_f g} x_6 x_7 \\ f_2 = \frac{-h}{2l} m_v x_6 + m_v \frac{l_r h}{le_f} x_8 - m_v \frac{h^2}{le_f g} x_5 x_8 \\ \quad - m_v \frac{h^2}{le_f g} x_6 x_7 \\ f_3 = \frac{h}{2l} m_v x_6 - m_v \frac{l_f h}{le_r} x_8 - m_v \frac{h^2}{le_r g} x_5 x_8 \\ \quad - m_v \frac{h^2}{le_r g} x_6 x_7 \\ f_4 = \frac{h}{2l} m_v x_6 + m_v \frac{l_f h}{le_r} x_8 + m_v \frac{h^2}{le_r g} x_5 x_8 \\ \quad + m_v \frac{h^2}{le_r g} x_6 x_7 \\ f_5 = x_6 \\ f_6 = 0 \\ f_7 = x_8 \\ f_8 = 0 \end{cases} \quad (10)$$

The observation model is linear and the output vector Z is presented as follows:

$$Z(t) = H \cdot X + \beta(t) \quad (11)$$

where $Z = [\Delta Fz_l\ (Fz_{fl} + Fz_{fr})\ a_x\ a_y\ \sum F_{ij}]$ and $\beta(t)$ is the measurement error, assumed to be white with zero mean:

- ΔFz_l is estimated from the second block;
- $Fz_{fl} + Fz_{fr}$ is calculated directly from (7);
- a_x is measured using an accelerometer;
- a_y is provided from the second block;
- $\sum F_{ij}$ is assumed to be equal to $m_v g$ at each instant.

The observation matrix H takes the form:

$$H = \begin{pmatrix} 1 & -1 & 1 & -1 & 0 & 0 & 0 & 0 \\ 1 & 1 & 0 & 0 & 0 & 0 & 0 & 0 \\ 0 & 0 & 0 & 0 & 1 & 0 & 0 & 0 \\ 0 & 0 & 0 & 0 & 0 & 0 & 1 & 0 \\ 1 & 1 & 1 & 1 & 0 & 0 & 0 & 0 \end{pmatrix}$$

The filter is initialized with the state vector:

$$X_0 = [m_{fl}g\ m_{fr}g\ m_{rl}g\ m_{rr}g\ 0\ 0\ 0\ 0].$$

6. OBSERVABILITY ANALYSIS

Observability is a measure of how well internal states of a system can be inferred by knowledge of its external outputs.

6.1 Linear system

The system described in section 4 is observable. Indeed, we have verified that the observability matrix O given by:

$$O = \left[C\ CA\ CA^2\ ...\ CA^5\right] \quad (12)$$

has a full rank.

6.2 Nonlinear system

In the nonlinear case, the observability definition is local and uses the Lie derivative method. The calculated rank of the observability matrix O, along the path, corresponded to the state vector dimensions, so the system described in section 5 is observable. In practice, for nonlinear systems, it seems reasonable to quantify the degree of observability with the observability index, defined as:

$$\Lambda(x) = \frac{\lambda_{min}\left[O^T O, x(t)\right]}{\lambda_{max}\left[O^T O, x(t)\right]} \quad (13)$$

where $\lambda_{max}\left[O^T O, x(t)\right]$ indicates the maximum eigenvalue of matrix $O^T O$ estimated at point $x(t)$ (likewise for λ_{min}). Then, $0 \leq \Lambda(x) \leq 1$, and the lower bound is reached when the system is unobservable at point x. (Stephant (2007); Aguirre et al. (2005)). The index defined in (13) represents the condition number of the observability matrix O. Fig.5 presents the inverse of the condition number of matrix O for the maneuver computed from data acquired while the vehicle is in motion.

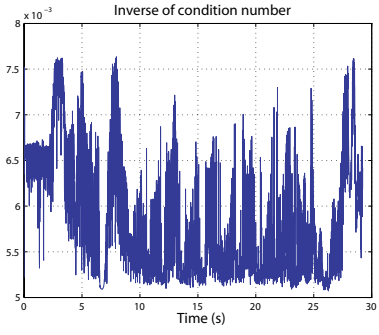

Fig. 5. Inverse of condition number of observability matrix.

7. EXPERIMENTAL RESULTS

The observers described in the sections above were evaluated by the advanced realistic vehicle simulation system CALLAS (see appendix A). The results of the simulation were very promising. After this validation in a simulated

environment, the observers were tested using experimental data.
The experimental vehicle shown in Fig. 6 is the INRETS-MA (Institut national de la recherche sur les transports et leur sécurité-département mécanismes d'accidents) Laboratory's test vehicle. It is a Peugeot 307 equipped with a number of sensors including accelerometers, gyrometers, steering angle sensors, linear relative suspension sensors with a precision of $0.0825mm$, and wheel force transducers. The developed observers were evaluated considering both

Fig. 6. Experimental vehicle

longitudinal and lateral dynamic behaviors as shown in Fig. 7. During the test, the vehicle first accelerated up to $0.3g$ then negotiated a slalom at a constant speed of $70km/h$, before it decelerated to $-0.7g$.

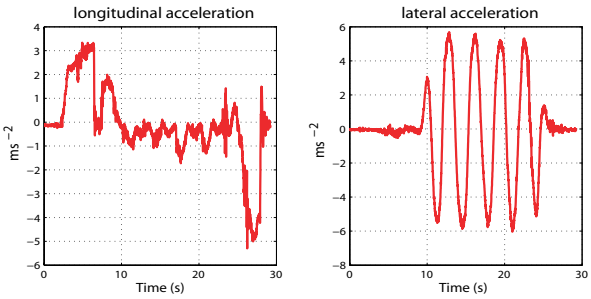

Fig. 7. Longitudinal and lateral acceleration.

All observers were implemented in a first-order Euler approximation discrete form. The sampling frequency is 100Hz. For our developed Kalman filters, error measurement covariance is determined by sensor variance and the error model covariance is determined by model quality.
The performance of the developed observers was caracterized by the normalized mean and normalized standard deviation (std). The normalized error is defined in Stephant (2007) as:

$$\epsilon_z = 100 \times \frac{\|z - z_{measured}\|}{max(\|z_{measured}\|)}$$

In the following, we propose to compare estimation results and real data. Table 1, Fig.8, Fig.9 and Fig.10 show the effectiveness of the observers. Indeed, observers produce satisfactory estimations close to the measured values (normalized mean and standard deviations error are less than 7%). Measured or reference data are shown in red. The estimated values are shown in dashed blue. Fig.8 represents the one-side lateral transfer load. It shows the convergence of the estimated values to their actual value in finite time. Fig.9 and Fig10 show the variation of the front and rear vertical load during the journey. The

	Max $\|\|\|$ (N)	Mean %	Std %
ΔFz_l	7309	4.42	4.6
Fz_{fl}	6386	2.8	2.7
Fz_{fr}	6212	2.5	2.4
Fz_{rl}	4906	2.4	2.3
Fz_{rr}	4862	2.3	2.4

Table 1. Maximum absolute values, normalized mean errors, and normalized Std.

estimated normal tire forces are satisfactory. These good results confirm that the presented algorithm is suitable.

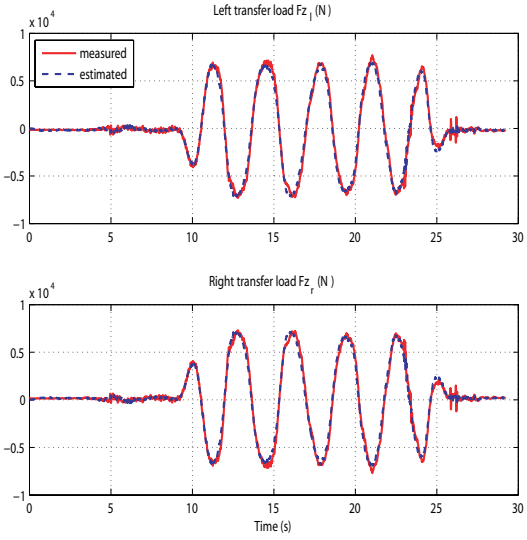

Fig. 8. Lateral transfer load.

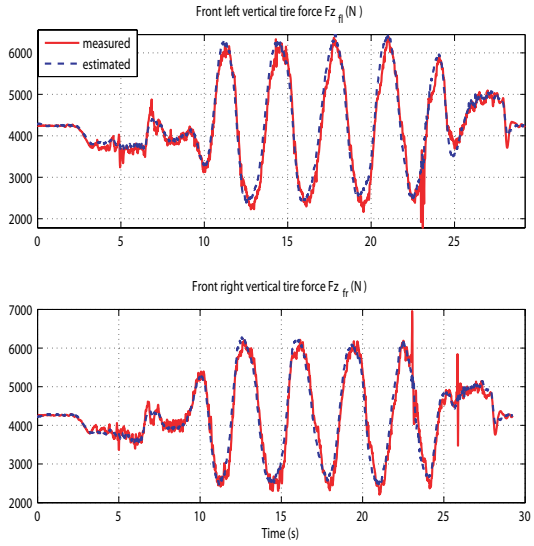

Fig. 9. Estimation of front vertical tire forces.

Fig.11 compares the LTR obtained from measured forces (plotted in red) with the LTR obtained from estimated forces (drawn in dashed blue). It can been seen that the estimated LTR fits the measured LTR well. Finally, Fig.12 illustrates the estimated LTR parameter with respect to roll angle obtained according to the measurements of the suspension relative displacement sensors. It is clearly seen

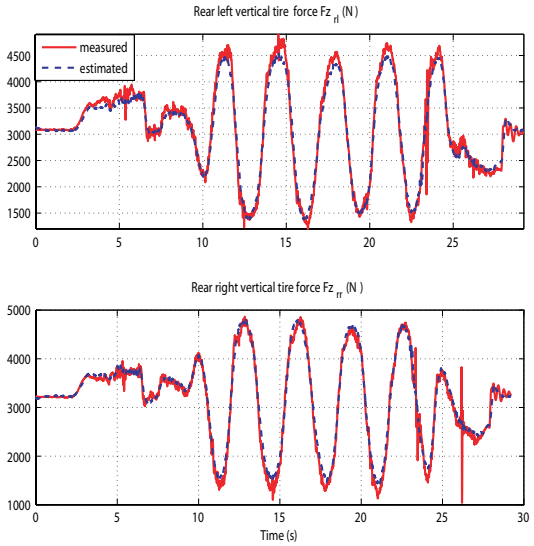

Fig. 10. Estimation of rear vertical tire forces.

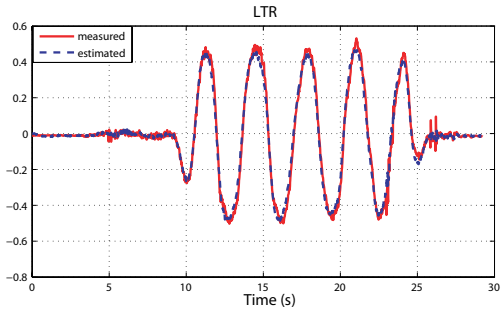

Fig. 11. Estmation of the LTR parameter.

that the relationship between the estimated LTR and the calculated roll angle is linear. When the suspension operates in linear mode, this relationship is obtained by combining equations (3) and (8).

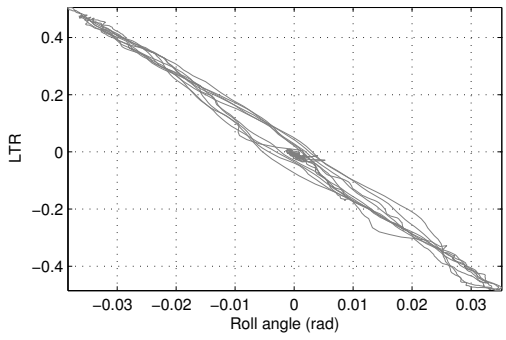

Fig. 12. Relation between LTR and roll angle.

8. CONCLUSIONS AND PROSPECTS

This paper has presented a new algorithm to estimate tire vertical forces, regardless of the tire model. Roll and combined longitudinal-lateral dynamics are elaborated to this end. Experimental results are presented to illustrate the ability of this approach to give estimation of vertical tire forces.
Although the identified mass tends toward the real mass value, the weak point of this approach is the determination of the vehicle's mass, which is highly dependent on the relative suspension sensors used. Moreover, the suspension model is linear, which does not correspond to the real case. We think that it should be possible to develop a model where the mass is considered as an internal state, and to initialize this state with our identification method. Future studies will take into account road angle and road irregularities.

REFERENCES

D. Lechner. *Analyse du comportement dynamique des vehicules routiers légers: développement d'une méthodologie appliquée à la sécurité primaire.* Ph. D, dissertation Ecole Centrale de Lyon, France, 2002.
T. Shim and C. Ghike. *Understanding the limitations of different vehicle models for roll dynamics studies.* Vehicle System Dynamics, volume 45, pages 191-216, March 2007.
U. Kiencke, L. Nielsen. *Automotive control systems.* Springer, 2000.
T.A. Wenzel, K.J. Burnham, M.V. Blundell and R.A. Williams. *Dual extended Kalman filter for vehicle state and parameter estimation.* Vehicle System Dynamics, volume 44, pages 153-171, February 2006.
A. Vahidi, A. Stefanopoulou and H. Peng. *Recursive least squares with forgetting for online estimation of vehicle mass and road grade: theory and experiments.* Vehicle System Dynamics, volume 43, pages 31-55, January 2005.
R.A. Anderson. *Using GPS for model based estimation of critical vehicle states.* Masters science thesis, Aubern University, Alabama, December 2004.
W.F. Milliken and D.L. Milliken. *Race car vehicle dynamics.* Society of Automotive Engineers, Inc, U.S.A, 1995.
T. Brown, A. Hac and J. Martens. *Detection of vehicle rollover.* SAE World Congress, Michigan-Detroit, March 2004.
N.V. RAO *An approach to rollover stability in vehicles using suspension relative sensors and lateral acceleration sensors.* Master science thesis, Texas A&M University, December 2005 .
F. Boettiger, K. Hunt and R. Kamnik. *Roll dynamics and lateral load transfer estimation in articulated heavy freight vehicles.* Proc.Instn Mech. Engrs Vol. 217 Part D: J. Automobile Engineering, 2003.
H. Durrant-Whyte. *Multi sensor data fusion.* Australian centre for field robotics, University of Sydney NSW 2006, January 2001.
L.A. Aguirre and C. Letellier. *Observability of multivariate differential embeddings.* Journal of Physics A: Mathematical and General, June 2005.
J. Stéphant, A. Charara and D. Meizel. *Evaluation of sliding mode observer for vehicle sideslip angle.* Control Engineering Practice. vol.15, pp. 803-812, July 2007.

Appendix A. CALLAS SOFTWARE

CALLAS software is a realistic simulator validated by vehicle manufacturers including PSA, and research institutions including INRETS. The CALLAS model takes into account vertical dynamics (tires, suspensions), tire adhesion, kinematics, elasto-kinematics and aerodynamics. This vehicle simulator was developped by SERA-CD (www.callasprosper.com).